View metadata, citation and similar papers at core.ac.uk
brought to you by CORE
provided by Texas A&M Repository

A PRIORI MODELING OF THERMAL RUNAWAY CONSEQUENCES IN LITHIUM-ION BATTERIES

An Undergraduate Research Scholars Thesis

by

RITIKA BHATTACHARJEE[1], CHRISTIAN A. LANDRY[2], AND ALEXIS A. COLE[3]

Submitted to the LAUNCH: Undergraduate Research office at
Texas A&M University
in partial fulfillment of requirements for the designation as an

UNDERGRADUATE RESEARCH SCHOLAR

Approved by
Faculty Research Advisors: Dr. Eric L. Petersen
Dr. James C. Thomas

May 2021

Majors: Chemical Engineering[1]
Mechanical Engineering[2]
Chemical Engineering[3]

Copyright © 2021. Ritika Bhattacharjee[1], Christian A. Landry[2], and Alexis A. Cole[3].

RESEARCH COMPLIANCE CERTIFICATION

Research activities involving the use of human subjects, vertebrate animals, and/or biohazards must be reviewed and approved by the appropriate Texas A&M University regulatory research committee (i.e., IRB, IACUC, IBC) before the activity can commence. This requirement applies to activities conducted at Texas A&M and to activities conducted at non-Texas A&M facilities or institutions. In both cases, students are responsible for working with the relevant Texas A&M research compliance program to ensure and document that all Texas A&M compliance obligations are met before the study begins.

We, Ritika Bhattacharjee[1], Christian A. Landry[2], and Alexis A. Cole[3], certify that all research compliance requirements related to this Undergraduate Research Scholars thesis have been addressed with my Research Faculty Advisors prior to the collection of any data used in this final thesis submission.

This project did not require approval from the Texas A&M University Research Compliance & Biosafety office.

TABLE OF CONTENTS

ABSTRACT

A Priori Modeling of Thermal Runaway Consequences in Lithium-Ion Batteries

Ritika Bhattacharjee[1], Christian A. Landry[2], and Alexis A. Cole[3]
Department of Chemical Engineering[1]
Department of Mechanical Engineering[2]
Department of Chemical Engineering[3]
Texas A&M University

Research Faculty Advisor: Dr. Eric L. Petersen
Department of Mechanical Engineering
Texas A&M University

Research Faculty Advisor: Dr. James C. Thomas
Department of Mechanical Engineering
Texas A&M University

Numerous experimental methods are available to predict the hazards associated with thermal runaway (TR) and subsequent catastrophic failure of lithium-ion batteries (LIB), but these methods are time-intensive and costly. The current study provides a thorough review of these experimental methods which include closed-vessel gas sampling, accelerating rate calorimetry, cone calorimetry, and Tewarson calorimeters. The strengths and weaknesses of each experimental method as applied by various researchers are critically analyzed, and several shortcomings of current approaches are identified. Key deficiencies in current approaches include lack of control of reactant gases (i.e., ambient air or similar), inadequate heating rates that are not comparable to realistic conditions, and failure to measure condensable reaction products (e.g., water or liquid electrolyte).

In lure of experimental approaches, an *a priori* modeling approach based on chemical equilibrium analyses (CEA) is proposed herein. Standard CEA software is limited in applicability, so that several improvements are required for accurate modeling. These improvements include prediction of electrolyte solutions densities; inclusion of key reactant and/or product species and their respective thermodynamic properties; and accurate representation of high-temperature oxygen release from metal oxide cathodes. The current study focuses on addressing the first of these two improvements, but additional work is still required to fully address them. Future work will encompass resolving the third improvement (i.e., metal oxide oxygen release), model validation against available experimental data, and modeling of LIB failure scenarios to inform future designs.

ACKNOWLEDGEMENTS

Contributors

We would like to thank our faculty advisors, Dr. James “Chris” Thomas and Dr. Eric L. Petersen, for their guidance and support throughout the course of this research. Thanks also go to our friends and colleagues and the department faculty and staff for making our time at Texas A&M University incredibly memorable. We would like to give a special thanks to our colleague, Cyndi G. Kunz, who helped tremendously with this thesis, but was not a part of the Undergraduate Research Scholars program.

The data and materials analyzed and used for **A Priori Modeling of Thermal Runaway Consequences in Lithium-Ion Batteries** were provided by James C. Thomas, Eric L. Petersen, Ritika Bhattacharjee, Christian A. Landry, Cyndi G. Kunz, and Alexis A. Cole. The analyses depicted in **A Priori Modeling of Thermal Runaway Consequences in Lithium-Ion Batteries** were conducted in part by the Turbomachinery Laboratory with the J. Mike Walker '66 Department of Mechanical Engineering and were published in 2021. All other work conducted for the thesis was completed by the student independently.

Funding Sources

There was no external funding for this research project.

NOMENCLATURE

LIB	Lithium-Ion Battery
TR	Thermal Runaway
ARC	Arc Cone Calorimetry
CEA	Chemical Equilibrium Analysis
SEI	Solid Electrolyte Interface
SOC	State of Charge

1. INTRODUCTION

Lithium-ion batteries (LIB) represent one of the most utilized electrochemical energy storage systems in the modern era with applications ranging from handheld electronics to automotive and aerospace vehicles. Damage from improper use, storage, or charging may cause LIBs to fail catastrophically via thermal runaway (TR) and/or subsequent combustion reactions. The potential hazards associated with such events include release of toxic gases, energy, and potentially combustible material. Several experimental approaches are currently utilized to evaluate such hazards, such as cone calorimetry, Tewarson calorimeters, accelerating rate calorimetry (ARC), and closed-vessel experiments with gas sampling. All of these experimental approaches can be time-consuming and expensive. Accordingly, the community would greatly benefit from an *a priori* modeling tool capable of predicting the type and severity of hazards associated with LIB TR and combustion. Chemical equilibrium analysis (CEA) is a modeling approach wherein the equilibrium product composition and thermodynamic state of a set of reactants are predicted by the minimization of free energy in conjunction with equilibrium reaction constants [1-2]. Furthermore, CEA represents a modeling approach that may be capable of *a priori* prediction of LIB TR and combustion hazards, including toxic gas release, gas temperature, and total energy release.

In the following section (Literature Review), LIB TR experimental efforts presented in the literature which are specifically aimed at characterizing TR hazards and gas emission are reviewed, where emphasis is placed on experiments with findings relevant to the modeling activities described herein. One key component of this effort is the exhaustive compilation of TR hazard experiments and relevant data from the literature into a concise and easily navigable set of tables

(**Tables 2.1-2.2**). In the subsequent section (Modeling Approach), the framework for the modeling approach adapted herein is described. In particular, a generic CEA approach is presented and intricacies related to CEA modeling of LIB TR are detailed. Modeling efforts will be benchmarked against available literature data for plain electrolytes, electrolyte/salt solutions, and LIB cells in future work. In addition, parametric studies will be conducted to elucidate potential compositional and environmental effects on LIB TR hazards, which should help inform future LIB designs and safety strategies. Finally, a summary, key findings, and relevant areas of future work are presented in the Conclusion section.

2. LITERATURE REVIEW

The physical hazards associated with LIB TR are relatively well documented and include the release of large amounts of thermal energy and emission of toxic and potentially combustible gases. A brief introduction to important phenomena associated with LIB TR is provided herein and the interested reader is referred to several notable reviews [3-4] for further information. Abuse of LIB systems by thermal (overheating or fire exposure), electrical (overcharging or deep discharging), or mechanical (crushing, penetrating, etc.) means can lead to conditions suitable for TR. In general, TR occurs when the heat generated by in-situ exothermic reactions is larger than heat dissipation to the surrounding environment. A generalized TR process diagram is shown in **Fig. 2.1**, where the energy release/consumption of specific components is plotted against temperature and shown for various cell chemistries. This process can be largely described in three steps: 1) anodic reactions occur and the SEI begins to decompose, leading to the local reduction of electrolyte; 2) exothermic reaction occur at the cathode yielding oxygen release; and 3) the cathode rapidly decomposes and the electrolyte rapidly decomposes/oxidizes. Decades of theoretical and experimental efforts presented within the literature have improved our knowledge of these complex and coupled phenomena, but our understanding is still fragmented and has considerable room for improvement.

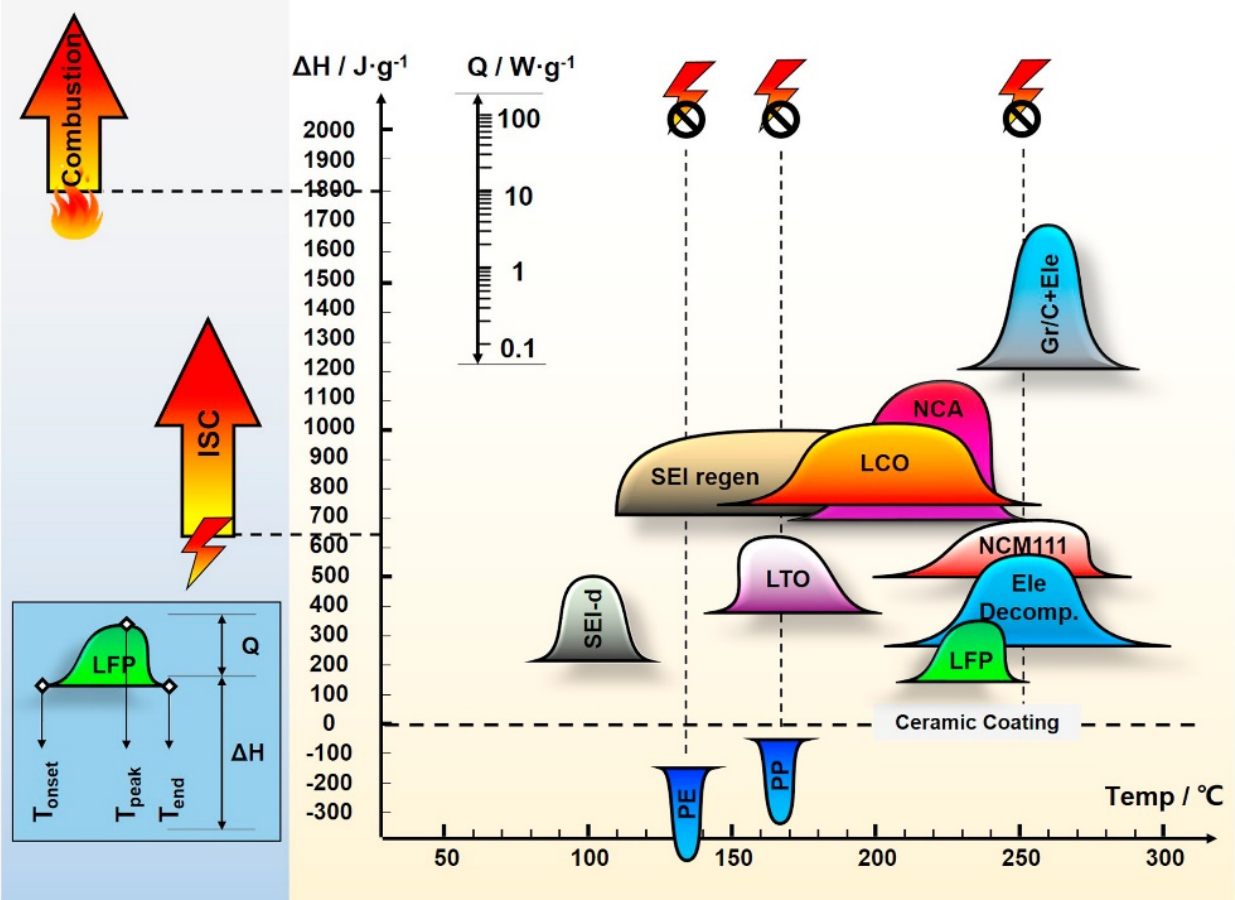

Figure 2.1. *Thermal description and energy release diagram for lithium-ion battery systems composed of a range of component chemistries. (Reprinted from Feng et al., 2018 [3] with permission. Permission located in Appendix A.)*

To the authors' knowledge, there is currently no theoretical modeling framework capable of predicting the consequences of LIB TR *a priori*. In an effort to elucidate the parameters that influence these consequences and inform such a modeling approach, the authors have conducted a thorough review of the relevant literature and experiments reported therein for electrolytes and LIB cells. A summary of these review efforts is given for plain electrolytes and electrolyte/salt solutions (**Table 2.1**), and single LIB cells and packs (**Table 2.2**) under a wide range of conditions and failure modes. The interested reader is referred to individual publications for further details. In the following sub-sections, key experimental efforts are highlighted, especially as they relate to the modeling efforts adapted here.

Table 2.1. *Summary of lithium-ion battery thermal runaway experiments reported in the literature for LIB cells. Details are provided regarding the cell chemistry, testing methods, and data collection.*

Reference	Cell			Electrolyte		
	Type	Chemistry	SOC (%)	Solvent	Salt	Concentration
Roth et al., (2004)	18650	N/A	N/A	PC:DMC	$LiPF_6$	Unknown
	18650	N/A	N/A	EC:DEC (1:1)	$LiPF_6$	1 mol/L
	18650	N/A	N/A	EC:EMC (3:7)	$LiPF_6$	1.2 mol/L
Abraham et al., (2006)	18650	NCA	100	EC:EMC (3:7 by wt)	$LiPF_6$	1.2 mol/L
Ribière et. al (2011)	Pouch	2.9 Ah (11 Wh) Pouch	0, 50, 100	EC:DEC:DMC	LiPF	1.2 mol/L
Wang et al., (2012)	18650, Pouch	LMO, LFP, LCO	N/A	N/A	N/A	N/A
Roder et al., (2013)	18650	N/A	50, 80, 100	EC:DMC (1:1)	$LiPF_6$, Li0FePO4	1 mol/L
Larsson et al., (2014)	Pouch or K2 26650	LFP	0, 50, 100	N/A	LiPF6	N/A
Eshetu et al, (2014)	N/A	N/A	N/A	EC:DMC, EC:DEC, EC:EMC, EC:DEC:DMC, EC:PC:DMC	LiPF6, LiFSI	N/A
Somandepalli et al., (2014)	Pouch	LCO	50, 100, 150	EC:DEC	N/A	N/A
Somandepalli & Biteau (2014)	Pouch	LCO	0, 50, 100	N/A	N/A	N/A
Golubkov et al., (2013)	18650	LCO/NMC	0,50,100	DMC : EMC : EC (6 : 2 : 1),	N/A	N/A
	18650	NMC	0,50,100	DMC : EMC : EC : PC (7 : 1 : 1 : 1)	N/A	N/A
	18650	LFP	0,50,100	DMC : EMC : EC : PC (4 : 2 : 3 : 1)	N/A	N/A
Golubkov et al., (2015)	18650	NCA	0-143	EC:DMC:EMD:PMC (17.1:49.7:5.4:2.7 %wt)	$LiPF_6$	3.1 mmol
	18650	LFP	0-143	EC:DMC:EMC:PC (24.8:33:16.5:8.3 %wt)	LiPF	4.9 mmol
Spray et al., (2015)	Pouch	LCO	0, 50, 100, 150	N/A	N/A	N/A
Liu et al., (2015)	18650	NMC	0, 25, 50, 100	Alkyl Carbonate	N/A	N/A
Liu et al., (2016)	18650	LCO, NMC, LFP	0, 25, 50, 100	N/A	N/A	N/A
Lecocq et al., (2016)	Pouch	LFP	0, 50, 100	EC:DC:DMC (1:1:3)	LiPF or LiFSI	1 mol.L
Sun et al., (2016)	18650, Pouch	spinel LiMn2O4, NMC, LiCoO2 & LiFePO4.	0, 50, 100, 150	N/A	N/A	N/A
Nedjalkov et al., (2016)	Pouch	NMC	N/A	EMC:EC	$LiPF_6$	N/A
Larsson et al., (2017)	Prismatic hard Al-can	LCO	0-100	N/A	LiPF	N/A
	Pouch or Cylindrical	LFP	0-100	N/A	LiPF	N/A
	Pouch	NCA-LATP	0-100	N/A	LiPF	N/A
	18650	Laptop Pack (Unspecificed)	0-100	N/A	LiPF	N/A
Spray et al., (2017)	Pouch	LCO	50, 100, 150	N/A	N/A	N/A
Diaz et. al, (2018)	18650, Pouch	LCO	0-100	N/A	$LiPF_6$	N/A
	18650	NMC	0-100	N/A	LiPF	N/A
Fernandes (2018)	26650	LFP	100	DMC:EMC:EC:PC (4:2.2:2.1:0.5)	LiPF	1 mol/L
Peng et al., (2019)	Pouch	LFP	0, 50, 75, 100	N/A	N/A	N/A
Said et al., (2019)	18650 3 x 4 Array	LCO, NMC, or LFP	50, 100	N/A	N/A	N/A
Lee et al., (2019)	Tenergy ICR 18650	LCO	50, 100	N/A	N/A	N/A
Lee et al., (2020)	Tenergy ICR 18650	LCO	100	N/A	N/A	N/A
Forestier et al., (2020)	Pouch	NMC	100	EC:DMC:EMC	LiPF	1 mol/L
	Pouch	NMC	100	EC:DMC:EMC with 2 wt% VC	LiPF	1 mol/L
	Pouch	NMC	100	EC:DMC:EMC with 2 wt% VC	LiPF and LiFSI	2/3 and 1/3 mol/L
Spray et al., (2020)	18650	N/A	100	N/A	Li-ion	N/A

Experiment								
Failure Type	Measured Off-Gases							Other Measurements
	Electrolyte	CO	CO	H	C_xH_y	HF	Other	
Thermal Abuse (ARC 280-400 C, Microcal 25-65 C)			•	•	•	•	Ar, Ethly Flouride, Propylene, Propane	HR/HF, Pressure, XRD Patterns, SOC Effects, Age Effects
Thermal Abuse (ARC 280-400 C, Microcal 25-65 C)			•	•	•	•	Ar, Ethly Flouride, Propylene, Propane	HR/HF, Pressure, XRD Patterns, SOC Effects, Age Effects
Thermal Abuse (ARC 280-400 C, Microcal 25-65 C)			•	•	•	•	Ar, Ethly Flouride, Propylene, Propane	HR/HF, Pressure, XRD Patterns, SOC Effects, Age Effects
Thermal Abuse ARC (T = 150 C Quenced to Room Temp)	•	•	•	•	•		N/A	XRD, XRS, Intensity, BE
Thermal Abuse, Terwarson Calorimeter(T = 660 to 1083 C)		•	•		•	•	CO , CO, THC, NO, SO , HCl, HF	Heat Release Rate (HRR), Heat of Combustion
Thermal Abuse & Penetration		•	•			•	NO, SO2 and HCl	FTIR, GC-MS, NMR
ARC							FePO4. $Fe_3Pe_2O_7$	XRD, Pressure, HR
Combustion (External Propane Flame)						•	POF_3	HRR, HF Mass Flow, Voltage
Thermal Abuse (Tewarson Calorimeter)		•	•		•	•	CH2O, HCN, NOx, SO2, etc.	HRR, EDX Analysis
Combustion Chamber (Thermal Ramp at 100 C/min)		•	•	•	•		N/A	GC-MS, Explosion Characteristics of Vent Gases
Cone Calorimetery		•	•	•			O	HRR, TER, Mass Loss
Thermal Abuse (Heat rate ~2 C/min until 220 C)			•	•	•	•	O_3, N	Mass Split of Cell Components, Temp, GC-MS
Thermal Abuse (Heat rate ~2 C/min until 220 C)			•	•	•	•	O , N	Mass Split of Cell Components, Temp, GC-MS
Thermal Abuse (Heat rate ~2 C/min until 220 C)			•	•	•	•	O , N	Mass Split of Cell Components, Temp, GC-MS
Thermal Abuse (Thermal Ramp at 2 C/min, Inert Atm)			•	•	•	•	O , N	Mass Split of Cell Components, OCV, SOC Effects, Temp
Thermal Abuse (Thermal Ramp at 2 C/min, Inert Atm)			•	•	•	•	O , N	Mass Split of Cell Components, OCV, SOC Effects, Temp
Calorimetry (ARC, Cell, Cone)		•	•		•		N/A	HRR, Total Energy, Ignitability of Material,Smoke Production Rate
Thermal Abuse (Copper Slug Battery & Cone Calorimetery)							O , N	HRR, Energy/Power Loss
Thermal Abuse (Copper Slug Battery Calorimetery)							N/A	Mass loss, Numerical Modeling, Electrical Energy Stored
Thermal Abuse (Tewarson Calorimeter)		•	•			•	SO , HCN, NOx, CH_2O, O_2	NDIR, FID, FTIR, HRR
Thermal Abuse (External Flame)			•	•	•	•	SO , COS, C_xH_yOz, C_xH_yNz, C_3H_9NO	GC-MS, IC
Penetrationn & Overcharge	•	•	•	•	•	•	Acrolein, COS, Ambient Air	GC-MS, QMS
Combustion (External Propane Flame)					•		PF_5, POF_3	FTIR, HRR, HF Mass Flow
Combustion (External Propane Flame)					•	•	PF , POF	FTIR, HRR, HF Mass Flow
Combustion (External Propane Flame)					•	•	PF , POF	FTIR, HRR, HF Mass Flow
Combustion (External Propane Flame)					•	•	PF , POF	FTIR, HRR, HF Mass Flow
Calorimetry (OC, CDG, Cone) & Overcharge		•	•	•	•	•	NH_3, COF_2, $COCl_2$, CH_3CHO	CFD Analysis, HRR, TER, Smoke Production Rate, FTIR
Thermal Abuse & Penetration		•	•	•	•	•	DC, EC, PC, DMC, HCl, Acrolein, COF2, Formaldehyde, etc.	Mass Loss, Contaminated Volume
Thermal Abuse & Penetration		•	•	•	•	•	DC, EC, PC, DMC, HCl, Acrolein, COF2, Formaldehyde, etc.	Mass Loss, Contaminated Volume
Thermal Abuse (Overcharge)		•	•	•	•		C2H5F, CH3OCH3,CH3OCHO,C2H5OH, etc.	HRR, Voltage, Current
Thermal Abuse (Fire Test)			•			•	SO , NO, NO , HCl	HRR, FTIR
Copper Slug Battery Calorimetry, Electric Heater		•	•	•	•	•	O , POF , THC	LFL, Mass Loss, Heat Gen
Copper Slug Battery Calorimetry		•	•	•			O_2, THC	LFL, Mass Loss, Heat Gen
Thermal Abuse (Electric Heater 115 W)		•	•	•			O , N , THC	Propagation speed, Heating rates
Thermal Abuse	•	•	•	•	•	•	SO , HCN, NOx, POF	FTIR
Thermal Abuse	•	•	•	•	•	•	SO , HCN, NOx, POF	FTIR
Thermal Abuse	•	•	•	•	•	•	SO , HCN, NOx, POF	FTIR
Thermal Abuse (from ~50 C at a rate of 5 C/min)		•	•	•	•		O , N , Ar	GC

Table 2.2. *Summary of lithium-ion battery thermal runaway experiments reported in the literature for plain electrolytes and electrolyte/salt solutions. Details are provided regarding the electrolyte or solution chemistry, testing methods, and data collection.*

Reference	Electrolyte		
	Solvent	Salt[b]	Concentration
Gavritchev et al., (2002)	HF	LiPF	N/A
Roth et al., (2004)	EC:DEC	$LiPF_6$	1 mol/L
	EC:EMC	$LiPF_6$	1.2 mol/L
	EMC, EC:EMC	$LiPF_6$	1.2 mol/L
Eshetu et al, (2014)	EC:DMC, EC:DEC, EC:EMC, EC:DEC:DMC, EC:PC:DMC	LiPF6, LiFSI	N/A
Lamb et al., (2015)	DEC, EC, EMC, DMC	$LiPF_6$	1.2 mol/L

Experiment								
Failure Type	Measured Off-Gases							Other Measurements
	Electrolyte	CO_2	CO	H_2	C_xH_y	HF	Other	
Thermal Abuse (Calorimetric Crucible)						•	LiF, PF_5	Enthalpy, Heat Capacity, DSC Curves
ARC Bomb, DSC	•						N/A	Rate (C/min) & Pressure (psi)
ARC Bomb, DSC	•						N/A	Heat Flow (cal/gs)
ARC Bomb	•						N/A	Rate (C/min) & Pressure (psi)
Thermal Abuse (Tewarson Calorimeter)		•	•		•	•	CH2O, HCN, NOx, SO2, etc.	HRR, EDX Analysis
ARC (405 C)		•	•	•	•		O_2, ethylether, Fluroethane, etc.	BP, Mole Ratio

2.1 US National Labs Collaboration Experiments (2006-present)

Researchers at several US national labs, and especially Sandia National Laboratories, have performed series of accelerating rate calorimetry (ARC) experiments with electrolyte solutions and LIB cells. Abraham et al. [6] evaluated 18650-type LIB cells in full and quenched ARC measurements. Detailed characterization of the cell chemistry and composition data are provided by Abraham et al. [6]; the cathode material was based on $LiNi_{0.8}Co_{0.15}Al_{0.05}O_2$ and the electrolyte solution was comprised of EC:EMC (3:7 wt%) with 1.2 M $LiPF_6$. LIB cells were charged to 100% state-of-charge (SOC) and subsequently heated to a) failure or b) 150 °C and air-quenched. Self-heating and exothermic decomposition of the anode was observed at a temperature of approximately 84 °C and was confirmed via scanning electron microscopy (SEM) imaging and X-ray photoelectron spectroscopy (XPS) analysis of the anode surface in the quenched cells. In general, the generated gas composition included CO_2 and CO, with smaller quantities of H_2, C_2H_4, CH_4, and C_2H_6.

Roth et al. [7] studied the decomposition, self-heating characteristics, and gas generation in LIB cells and components under abuse conditions through interrupted ARC and differential scanning calorimetry (DSC) experiments. Investigated cells included commercial cell chemistries (SONY 1.2 A-h 18650 LCO) and custom cells with well-defined compositions. Roth et al. [7] determined the TR process was well described by three stages: Stage 1 (< 125 °C) indicated the onset of thermal runaway, Stage 2 (125 – 180 °C) involved venting and accelerated heating, and Stage 3 (> 180 °C) referred to explosive decomposition. In the first stage, exothermic solid electrolyte interphase (SEI) decomposition reactions take place at the anode surface, yielding electrolyte reduction and gas generation which increases with temperature. In the second stage, decomposition of the electrolyte and gas generation continue to increase in severity, and the

cathode begins to break down. In the final stage, a rapid increase in heat and gas generation is observed alongside explosive decomposition. One significant achievement of this work was the establishment of a rich database of vent gas compositions for experiments interrupted at several intermittent temperatures, which also includes detailed initial cell chemistries.

In a similar work, Lamb et al. [8] performed interrupted ARC experiments with various LIB electrolyte solvents (EC, DEC, EMC, and DMC) and salt ($LiPF_6$) solutions. Gas production and composition were determined via gas chromatography mass spectroscopy (GC-MS). Lamb et al. [8] observed that EC and DEC were the most significant contributors to total gas production, and DMC was somewhat stable in all cases. Although significant quantities of toxic gases were not observed, the decomposition gasses themselves all comprised potentially combustible mixtures.

Nagasubramanian et al. [10] evaluated "baseline" electrolytes which consist of either EC:EMC (3:7 wt. %) and 1.2 M $LiPF_6$ or EC:DEC (5:95 vol.%) and 1 M $LiPF_6$ as electrolytes in comparison to hydrofluoroether (HFE) cosolvent electrolytes in 18650 cells. Nagasubramanian et al. [10] discovered electrolytes with HFE have the best safety factor. Flammability and ARC testing showed the HFE electrolytes exhibited non-flammability characteristics and released less gas. For instance, the volume of gas released by HFE electrolytes was approximately half that of the baseline electrolyte, but the HFE electrolytes also had an onset temperature of ~160 °C while the baseline's was ~240 °C.

2.2 Exponent, Inc. (2014-present)

Researchers at Exponent, Inc. [12-15] have designed numerous experiments aimed at gaining a better understanding of the potential consequences of LIB TR and the factors that influence these. Somandepalli et al. [12] utilized cone calorimetry experiments to evaluate the heat

release rate and total heat release of 2.1 A-h pouch cells (LCO) with varying SOC (0, 50, and 100%), where the cell composition was also thoroughly characterized. Somandepalli et al. [12] noted the heat release rate increased with the cell's SOC and hypothesized this finding was associated with the lithiated cathode more readily releasing oxygen. Somandepalli et al. [13] evaluated the same cells in a closed-volume vessel filled with inert gas (Ar) where emission gases (CO_2, CO, H_2 , and hydrocarbons) were characterized with GC-MS techniques. Larger volumes of gas emission were observed for higher cell SOCs and more CO production was noted. Somandepalli et al. [13] compared their collected gas composition to those of Roth et al. [17] and noted several stark differences, and attributed these to experimental differences including electrolyte composition, cell format (18650 versus pouch), and heating rate. Somandepalli et al. [13] suggested the last difference was most important and that their implied heating rates from resistance heaters (~100 K/min) were more representative of realistic conditions in comparison to slower heating rates typically employed in ARC experiments. Spray et al. [14] extended the work of Somandepalli et al. [12-13] to also include transient gas analysis for a cell exposed to overcharging conditions with FTIR techniques.

Spray et al. [14] conducted ARC experiments examining the self-heating onset temperatures (SHOT) for TR and temperature-dependent self-heating rates (SHR) for various cell chemistries (NCM, LCO, and LFP), as shown in **Fig. 2.2**. The SHOTs were observed to be both chemistry and SOC dependent, where the apparent SHOTs decreased with increasing SOC. Interestingly, Spray et al. [14] found that the SHRs for a given temperature above the SHOT were generally comparable across all evaluated chemistries and scaled will cell energy, as shown in the plot on the right in **Fig. 2.2**.

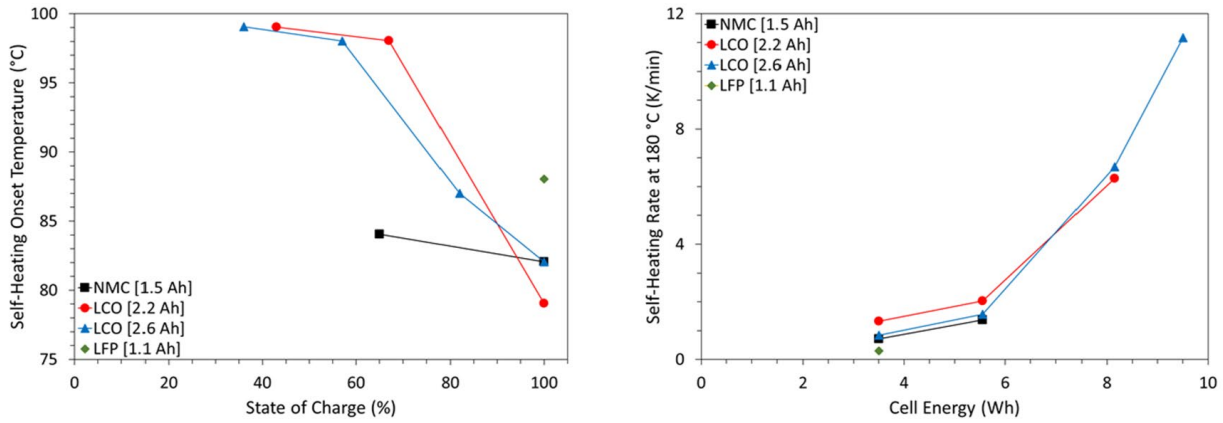

Figure 2.2. *Thermal stability of LIB cells with varying cathode chemistries and SOCs as measured during ARC experiments by Spray et al. [14].*

Recently, Spray et al. [16] presented a parametric study on the effects of ambient gas (air versus N_2) and vessel size (6 versus 60 L) on the resultant LIB TR gas emission composition in closed vessel experiments similar to those of Somandepalli et al. [13]. All of the available oxygen was consumed for the small-vessel combustion case (6 L, air), but not for the similar large-vessel case (60 L, air). Furthermore, the small-vessel case had correspondingly lower CO_2, higher CO, and higher total hydrocarbon concentrations. These observations were consistent with TR vent gas burning with the ambient O_2 in a fuel-lean (oxygen-rich) condition, yielding more complete combustion. Interestingly, a 160% larger total gas volume production was noted for the large-vessel inert case (60 L, N_2) in comparison to the large-vessel combustion case (60 L, air). However, Spray et al. [16] logically noted that this finding may be linked to the lack of evaluation of condensable gases in their experiment, especially H_2O, since gas sampling is completed after the system has cooled.

2.3 French Collaboration Contributions (CNRS, INERIS, et al.) (2012-present)

Eshetu et al. [18-19] utilized a Tewarson calorimeter coupled with FTIR gas analysis to measure transient mass loss, heat release rate, and gas emission for neat electrolytes (EC, DMC,

DEC, EMC, PC, and EA) and electrolyte solutions with and without salts ($LiPF_6$ or LiFSI) undergoing forced combustion. Although Tewarson calorimeters are useful for measuring fundamental combustion parameters, such as the effective heat of combustion (ΔH_c), their lack of direct control of bath gas volume for the entire reaction make the modeling approach adapted herein incompatible. Measured values for electrolyte ΔH_c, particularly in an oxygen rich environment, agreed well with those predicted by the Dulong correlation [20] or the Boie correlation [21] developed to predict higher heating values of coals and fuels/oils, respectively, based on their atomic composition. Furthermore, Eshetu et al. [18-19] emphasized the correlation of electrolyte ΔH_c, to their atomic composition, as demonstrated in **Fig. 2.3**. Interestingly, the addition of lithium salts to the electrolyte solutions did not significantly affect the observed heat release rates or effective heat of combustion. In comparison to the $LiPF_6$, electrolyte solutions containing LiFSI exhibited a decrease in HF gas evolution, but with an accompanying increase in other toxic gases, such as SO_2, which could exacerbate the toxicity hazards. Similar results were reported for a follow-on study by Lecocq et al. [22]. Eshetu et al. [19] also notably produced a set of electrolyte solvent screening guideline for maximum safety and provided a comparative ranking of the evaluated electrolytes, of which EC was deemed the best for its safety properties.

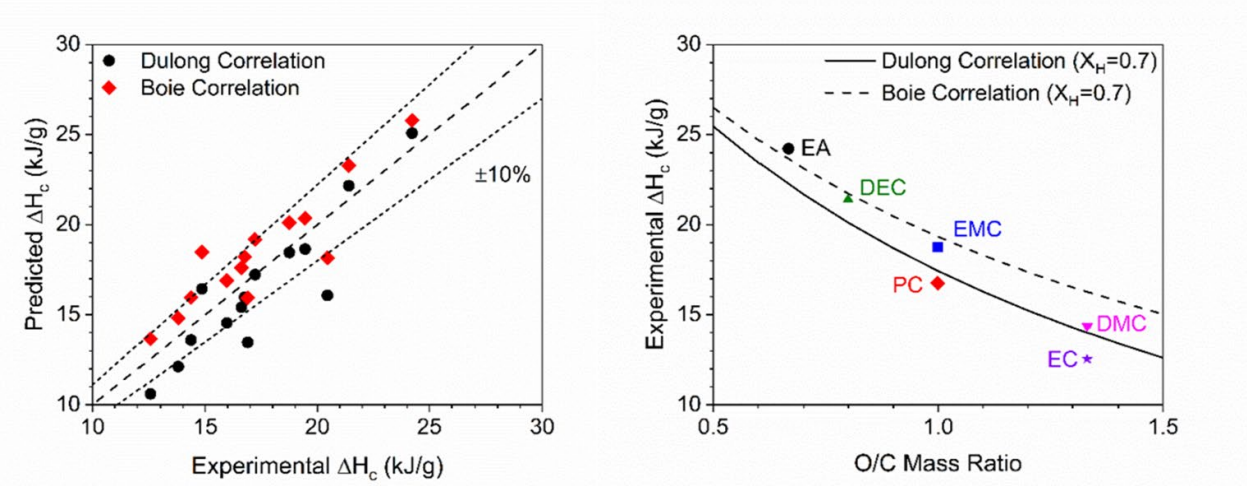

Figure 2.3. *Correlation of predicted heat of combustion and atomic composition for common LIB electrolytes. (left) Demonstration of good agreement from measured heats of combustion [19] and predicted values [20, 21] for neat and mixed electrolytes. (right) Variation of neat electrolyte heat of combustion with oxygen-to-carbon mass ratio.*

Ribiere et al. [23] utilized a Tewarson calorimeter to analyze the mass loss characteristics, heat release rate, vent gas emissions, and total ΔH_c of 2.9 A-h pouch cells ($LiMn_2O_4$) undergoing TR at various SOCs (0, 50, and 100%). The total mass loss was nearly identical to the mass of organic compounds in the cell for all SOCs evaluated therein. Accordingly, Ribiere et al. [23] observed the cell's ΔH_c could be accurately estimated by summation the individual ΔH_c for all polymers (packaging, binder, and separator) and the electrolyte. The maximum observed values for toxic gases (CO, NO, HCl, SO_2, and HF) were all well below 'safe' exposure limits for the single-cell experiments, but Ribiere et al. [23] noted cumulative gas concentrations from TR of larger battery packs could realistically yield unsafe conditions. Most recently, Forestier et al. [24] evaluated 0.6 A-h pouch cells (NMC) with and without vinylene carbonate (VC) electrolyte additives to stabilize and reinforce SEI formation at the anode/electrolyte interface. The presence of VC increased the onset temperature for thermal runaway (~20 °C), but did not significantly affect the amount or composition of gas emissions.

2.4 Golubkov et al. (2014, 2015)

Golubkov et al. [25] induced LIB TR in a pressure-tight, inert reactor by heating consumer 18650-type cells with several cathode chemistries (LFP, NMC, or LCO/NMC) at a SOC of 100%. Golubkov et al. [25] notably provided a detailed and thorough characterization of the cells prior to TR experiments, which is generally lacking in the literature and important for modeling purposes. Cell surface temperatures were measured, and vent gas compositions were analyzed with GC-MS methods. Golubkov et al. [25] observed that the LFP cells were the most thermally stable, exhibited TR at the highest temperature (195 ± 8 °C), and produced the least amount of vent gas. In contrast, the LCO/NMC cells were the least stable, exhibited TR at the lowest temperature (149 ± 2 °C), and produced the most amount of gas. These findings were expected, as the observed increasing thermal stability trend (LFP > NMC > LCO/NMC) corresponded to the decreasing stored electrical energy of each cell (i.e., they are inversely related). Golubkov et al. [25] also noted that all cells released appreciable amounts of flammable gases including significant proportions of hydrocarbons, and provided some theoretical discussion into the sources of each constituent gas.

Golubkov et al. [26] further investigated the effects of SOC (0 – 143%) with consumer 18650 LFP and NCA cells in the same experimental apparatus. Once again, cell compositions were thoroughly characterized prior to TR experiments. Golubkov et al. [26] observed that the cells needed to be charged above some threshold SOC to induce TR. Furthermore, increasing the cell's SOC yielded a reduction in the TR onset temperature, an increase in the maximum temperature reached, and an increase in gas production. In comparison to the NCA cells, the LFP cells exhibited superior thermal stability.

2.5 Swedish Collaboration Contributions (2014-2018)

Larsson et al. [27-29] quantitatively measured heat release rates and gas emissions (HF) for cells with various chemistries (LCO, LFP, and NCA/LATP) and geometries (18650, pouch, and pack) undergoing TR initiated with a propane burner. For the LFP pouch cells, Larsson et al. [28] demonstrated that increasing the cell SOC (0-100%) resulted in higher heat release rates, and also yielded quicker but similar HF production. The observed total heat release (15-75 kJ/W-h), heat release rates (80-730 W/W-h), and total HF gas emission (15-200 mg/W-h) was largely dependent on the cell type evaluated in their experiments. Larsson et al. [28] also found that appreciable amounts of another potentially toxic intermediate gas (phosphoryl fluoride, POF_3) were emitted during LIB TR.

2.6 University of Maryland (2015-present)

Liu et al. [30-31] developed a copper slug battery calorimetry (CSBC) experiment capable of measuring the internal heat generation of LIB cells undergoing forced TR. Furthermore, the CSBC was coupled with a cone calorimeter to measure the energy released in the vent gas and its subsequent reaction. As expected, experiments with 2.2 A-h 18650 cells (NMC) indicated increasing the cell's SOC led to larger energy releases [30]. Liu et al. [30] also observed that the total mass loss of the cell was directly linked to the how much energy was released in the cell versus in the gas emission and reaction. Liu et al. [31] utilized the same experiment to evaluate 18650 cells with different cathode chemistries (LCO, NMC, and LFP). Regarding internal heat generation, the LCO and LFP cells released the least energy. However, NMC cells released the most heat from gas emission and combustion, but only at higher SOCs (>50%).

In a recent effort, the same research group has developed a wind tunnel experiment in which arrays of 18650 cells are subjected to TR initiation and propagation [32-35]. The unique

experimental set-up allows for control of gas composition and flow rate over the cell array; includes diagnostics for vent/combustion gas sampling and analysis; and is particularly useful for studying TR propagation under controlled conditions. However, similar to the Tewarson calorimeter and the previously discussed copper slug calorimetry experiment, the lack of direct control of bath gas volume for the entire reaction period makes the modeling approach adapted herein incompatible with these experiments. Most notably, Said et al. [35] observed particular cathode chemistries (LCO > NMC > LFP) to emit larger amounts of flammable vent gases during TR, yielding an increase in TR propagation propensity and speed.

2.7 Other Notable Contributions

Sun et al. [36] analyzed the products released by commercial 18650-type and pouch cells with various cathode chemistries (LMO, NMC, LCO, and LFP) and SOCs (0-150%) which were directly ignited by a flame to initiate TR. More than 100 species of organic compounds were detected by GC-MS methods; CO levels were monitored by a multi-gas monitor; several gases (CO_2, PO_x, and HF) were monitored by solution saturation techniques and ion chromatography; and special attention was paid to potentially toxic effluents. NMC and LFP cells exhibited the most oxygen and HF release, respectively. However, the electrolytes varied amongst the evaluated cells and were not specified, so a direct comparison between the results obtained for different cathode chemistries is not possible within the dataset provided by Sun et al. [36].

Nedjalkov et al. [37] analyzed gas emissions from 40 A-h NMC pouch cells undergoing penetration-induced TR with various spectroscopic and wet analytical techniques. Most notably, Nedjalkov et al. [37] observed HF concentrations (1640 ppm) that were 50 times higher than the immediately dangerous to life or health (IDLH) limit.

Fernandes et al. [38] initiated TR in 2.5 A-h 26650 cells (LFP) via overcharging in a closed vessel filled with air and analyzed the gas emissions with GC-MS and FTIR techniques. A thorough description of the cell composition was determined through various experiments and provided. Temperature data collected via thermocouples attached to the cell tabs and video analysis suggest the cell(s) underwent TR, but not necessarily full combustion. Regardless, a rich dataset of various gas emissions (DMC, EMC, HF, CO_2, CO, H_2, CH_4, C_2H4, C_2H_5F, CH_3OCH_3, CH_3OCHO, C_2H_5OH, CH_3F, C_2H_6, PF_3, C_3H_6, and CH_3OH) was provided by Fernandes et al. [38] for a well-characterized experiment.

Diaz et al. [5] initiated TR (thermal or penetration) in commercially available LIB cells contained within a closed vessel filled with air or N_2 and analyzed the gas emissions with various techniques (FTIR, O_2 and H_2 analyzers, wet IC and ICD analysis). Evaluated cells included two 18650-type (LCO, NMC) and four pouch cells (LCO, NMC, LFP) at variable SOC (0, 50 or 100%). Diaz et al. [5] observed lower amounts of total gas emission, but higher amounts of toxic gas emission in penetration-induced TR experiments, in comparison to thermally-induced TR. Gas toxicity was generally higher for pyrolysis TR conditions (in N_2) versus combustion TR conditions (in air), while the total heat release is generally associated with the opposite trend. In general, LFP cathodes are regarded as the 'safest' choice due to their lower propensity for TR, but Diaz et al. [5] argued the observed higher toxicity of their corresponding TR emission gases, especially fluorides and chlorides, may negate this feature. However, Diaz et al. [5] also noted that this finding may be linked to the variable electrolytes and additives utilized within the different cells.

Peng et al. [39] analyzed the thermal-induced TR of 68 A-h pouch cells (LFP) in a cone calorimetry system with heat flux sensors and gas sampling techniques (FTIR, NDIR, and PA). Similar to other investigators, Peng et al. [39] found that increasing the cell's SOC yielded higher

total heat output, higher heat release rates, and more toxic gas emissions. However, in contrast to other investigators, Peng et al. [39] observed that several irritant gases (HF, SO_2, NO, NO_2, and HCl) were above the suggested OSHA thresholds for human exposure.

2.8 Summary

In the preceding sub-sections, the literature regarding LIB TR experiments and corresponding hazard characterization was reviewed in detail. In general, research efforts have focused on three types of experiments: ARC, cone or Tewarson calorimetry, and closed-vessel TR with gas-sampling. ARC experiments are highly controlled and can provide useful information regarding critical temperatures and decomposition at user-specified conditions. Direct control over the volume and composition of ambient gas makes these experiments ideal for modeling validation, but the slow heating rates generally imposed do not generally reflect realistic conditions. Cone or Tewarson calorimetry experiments do not include direct control over the volume of ambient gas that the electrolyte or cell being studied is allowed to react with, so that they are not suitable for the modeling via the approach adapted herein. However, these types of experiments can provide fundamental measurements, such as heat of combustion. Closed-vessel TR experiments represent the most realistic experimental approach available, especially when high heating rates are applied, and also allow for direct control of the ambient gas. Unfortunately, one aspect that is typically missing from all of these experimental studies, with only a few exceptions, is a thorough characterization of the cell composition prior to TR experiments.

Studies conducted with various electrolytes and electrolyte/salt solutions have shown that the corresponding decomposition and TR behavior in LIB cells can be highly dependent on the composition of these components. More explicitly, electrolyte thermal stability varies widely and the total energy release from their decomposition is strongly correlated to their atomic

composition. In general, the thermal stability of cells containing common electrodes follows the descending relative ranking: LFP > NMC > LCO. Furthermore, for a single cell chemistry, increasing the SOC yields a corresponding increase in total energy release and gas emission during TR. However, the total energy release appears to be strongly correlated to the total stored cell energy, more so than the cell chemistry.

Experimental efforts aimed at evaluation of the vent gas composition have mostly been compromised of GC-MS, FTIR, and wet analytical techniques. These efforts have primarily focused on evaluation of several key species (CO_2, CO, H_2, O_2, and hydrocarbons), while some authors have focused on toxic gases, such as HF or POF_3. One aspect that is clearly missing from these studies is the analysis of condensable gases formed during TR, such as water or residual liquid electrolyte.

3. MODELING METHODS AND APPROACH

As previously noted, the battery community does not currently posses a modeling tool capable of predicting the consequences of LIB TR *a priori*. Accordingly, the authors propose utilizing CEA modeling to fill this knowledge gap and relevant methods are discussed herein. CEA modeling approaches predict the equilibrium product composition and thermodynamic state of a set of reactants by minimizing the free energy in conjunction with equilibrium reaction constants [1-2]. These methods require an extensive set of thermodynamic data for all potential product species and phases. In addition, modeling inputs include the relative mass and molar concentration of all reactants, their initial thermodynamic state (i.e., pressure and/or temperature), and their standard heats of formation. The following sections detail approaches developed herein to estimate these inputs where they are missing, as well as highlight other intricacies related to CEA modeling of LIB systems. In addition, the current status of our modeling efforts is summarized and presented with a path forward.

3.1 Estimation of Electrolyte Solution Densities

Inputs into CEA computations include fully defined mass and molar concentrations of each constituent ingredient. Accordingly, one parameter of particular interest in the modeling approach developed herein is the density of electrolyte/salt solutions. A comprehensive review of the relevant literature revealed that applicable electrolyte solution density data (i.e., $LiPF_6$ in standard electrolytes) is limited to a few experimental measurements [40-43,46-47] and numerical estimations [44-45], and data provided by distributors for select solutions (i.e., Sigma Aldrich and Solvionic). The data for single electrolyte and $LiPF_6$ solutions, which comprises most of the entire dataset, is shown in **Fig. 3.1**. The scarcity of these data limit could potentially limit the extensions

of the CEA modeling approach to electrolytes and LIB cells containing those electrolytes where density data is already available. Accordingly, an electrolyte solution density estimation method was developed to circumvent this limitation.

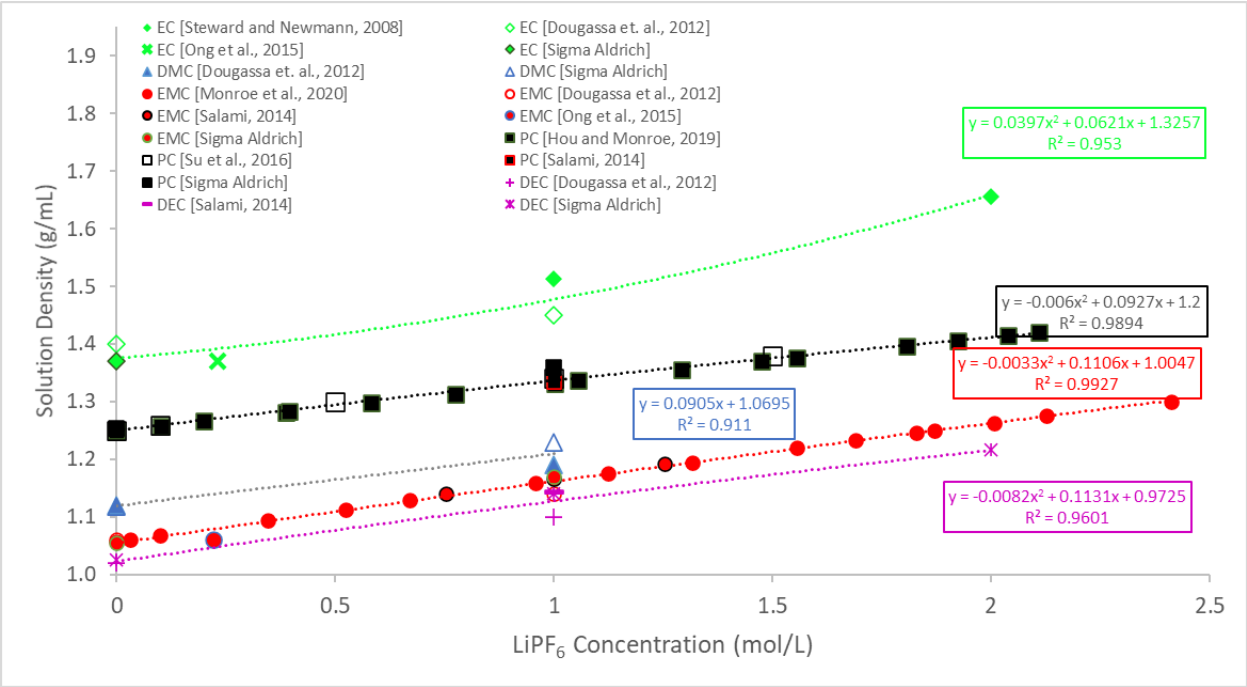

Figure 3.1. *Compilation of single electrolyte solution densities provided within the literature.*

Horsak and Slama [49] developed a model to predict the densities of 1:1 aqueous electrolyte solutions containing a wide variety of salts based on the concept of apparent molar volume and a compilation of density measurements. Lam et al. [48] extended this model to account for multicomponent ionic solutions with a wide variety of salts. A similar model is utilized herein for the prediction of LIB electrolyte solution densities. The solution density is given by:

$$\rho = \frac{\sum_{i=1}^{N_{ion}} x_i M_i + (1-\sum_{i=1}^{N_{ion}} x_i) M_{Electrolyte}}{\sum_{i=1}^{N_{ion}} v_i^o * x_i + v_{Electrolyte}^o * \left(1-\sum_{i=1}^{N_{ion}} x_i\right) + \sum_{i=1}^{N_{ion}} \alpha_i * x_i * (1-\sum_{i=1}^{N_{ion}} x_i)} \qquad (3.1)$$

where x_i, M_i, and v_i^o denote the molar fraction, molecular weight, and initial molar volume of each constituent component, respectively. An empirical interaction parameter (α_i) accounts for the change of the molar volume of neighboring electrolyte molecules with respect to each ion in the

salt. This parameter is empirically determined by fitting **Eq. (3.1)** to the experimental data previously described (**Fig. 3.1**). In the current representation, the empirical interaction parameter value for the Li^+ ion is taken as the value provided by Lam et al. [48] (0.0655 cm^3/mol), and single solution density data are fitted for each electrolyte to yield a series of PF_6^- interaction parameters specific to each electrolyte.

Electrolyte solution density modeling estimates are plotted in **Fig. 3.2** against the available data. Good agreement is noted between the model and literature data, but the model generally overpredicts solution densities at higher salt concentrations. The density prediction model is currently being further refined by considering variable Li+ interaction parameters unique to each electrolyte. In addition, future work will include extension of the current prediction capabilities to multi-component electrolyte solutions. The final version of the model should prove capable of accurately predicting the density of single and multiple component $LiPF_6$/electrolyte solutions over a range of salt concentrations.

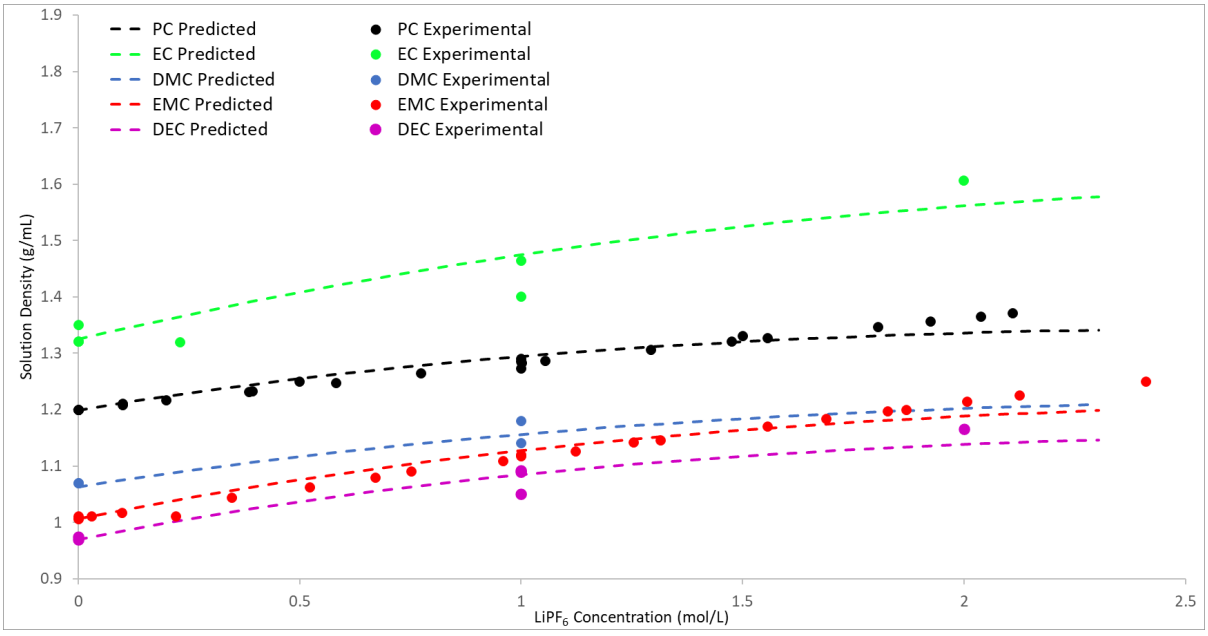

Figure 3.2. *Comparison of electrolyte solution density model predictions to data available in the literature for single electrolyte mixtures.*

3.2 Component Heats of Formation

Another necessary input for CEA modeling efforts is the heats of formation of all potential reactants. In general, the heats of formation of compounds are experimentally measured, but modern chemistry methods allow for accurate prediction for a wide variety of compounds. **Table 3.1** summarizes the relevant heat of formation data for standard electrolytes and LiPF6 taken from literature. Future modeling efforts considering full LIB cells and not just their electrolyte solutions will require additional data, but these are not considered herein.

Table 3.1. *Chemical and thermodynamic information for common electrolytes and salts utilized in lithium-ion battery applications. Data include molecular weight, density, and heat of formation.*

Electrolyte Ingredient		MW (g/mol)	ρ (g/cm^3)	ΔH_f^0 (kJ/mol)	Reference
Ethylene Carbonate (EC)	$C_3H_4O_3$	88.06	1.321	-531 ± 12	NIST Database
Dimethyl Carbonate (DMC)	$C_3H_6O_3$	90.08	1.069	-608.76 ± 0.14	NIST Database
Diethyl Carbonate (DEC)	$C_5H_{10}O_3$	118.13	1.006	-681.58 ± 0.56	NIST Database
Ethyl Methyl Carbonate (EMC)	$C_4H_8O_3$	104.10	0.975	-644 ± 13	NIST Database
Propylene Carbonate (PC)	$C_4H_6O_3$	102.09	1.204	-614.1 ± 3.4	NIST Database
Lithium Hexafluorophosphate	$LiPF_6$	151.91	1.50	-2296 ± 3	Gavritchev et al. [40]

3.3 Missing Thermodynamic Data

In general, commercial and freely available CEA software includes thermodynamic data for thousands of potential product species over a wide range of temperatures. These data include the molecular formula, molecular weight, density, and heat of formation of each species, as well as the temperature-dependent constant-pressure specific heat capacity, total enthalpy, and entropy. The temperature-dependent properties are typically provided as a series of nine fitted coefficients

for a temperature interval, and for several temperature intervals. The temperature-dependent properties are typically fitted to the NASA polynomial forms:

$$\frac{C_p^0}{R} = a_1 T^{-2} + a_2 T^{-1} + a_3 + a_4 T + a_5 T^2 + a_6 T^3 + a_7 T^4 \quad (3.2)$$

$$\frac{H^0}{RT} = \frac{\int C_p^0 dT}{RT} = -a_1 T^{-2} + a_2 \ln(T) + a_3 + a_4 \frac{T}{2} + a_5 \frac{T^2}{3} + a_6 \frac{T^3}{4} + a_7 \frac{T^4}{5} + \frac{a_8}{T} \quad (3.3)$$

$$\frac{S^0}{R} = \int \frac{C_p^0}{RT} dT = -a_1 \frac{T^{-2}}{2} - a_2 T^{-1} + a_3 \ln(T) + a_4 T + a_5 \frac{T^2}{2} + a_6 \frac{T^3}{3} + a_7 \frac{T^4}{4} + a_9 \quad (3.4)$$

In many cases, relevant product species are not already contained within the thermodynamic databases of CEA software and must be estimated by alternative means. For instance, most LIB electrolytes are not contained therein, but do represent potential product species, so they must be added. The temperature-dependent, gas-phase, specific heat-capacities of five common electrolytes (EMC, EC, PC, DMC, and DEC) were estimated herein with the 'Joback' group additive method, originally developed by Joback and Reid [54], which estimates the effects of atomic groups with a molecule on overall thermodynamic properties (e.g., heat of formation, Gibbs free energy of formation, boiling point, specific heat capacity, etc.). For example, the temperature-dependent specific heat capacity is given by:

$$c_p = A + BT + CT^2 + DT^3 \quad (3.5)$$

where A, B, C, and D represent the coefficients determined by group contributions ($A = \sum a_i - 37.93$, $B = \sum b_i + 0.210$, $C = \sum c_i - 3.91 \times 10^{-4}$, and $D = \sum d_i - 2.06 \times 10^{-7}$) and the individual contribution terms ($\sum a_i$, $\sum b_i$, $\sum c_i$, and $\sum d_i$) are tabulated for each group. The group additive constants only rely on the presence and number of chemical structures within a molecule, and relevant structures for the electrolytes of interest herein are shown in **Table 3.2**.

Table 3.2. *Chemical and thermodynamic information for common electrolytes and salts utilized in lithium-ion battery applications. Data include molecular weight, density, and heat of formation.*

Electrolyte	- CH_2 - (ring)	- CH_2 - (non-ring)	- CH_3 - (non-ring)	- O - (non-ring)	- O - (ring)	> C = O (non-ring)	> C = O (ring)
EMC	-	1	2	2	-	1	-
EC	2	-	-	-	2	-	1
PC	1	-	1	-	2	-	1
DMC	-	-	2	-	2	1	-
DEC	-	2	2	2	-	1	-

Relevant group contribution values were taken from the VDI Atlas [55] herein and utilized to estimate the specific heat capacities of relevant electrolytes. The computed temperature-dependent specific heat capacities are shown in **Fig. 3.3** and follow the expected trend of increasing with temperature. Predictions are only computed to a temperature of 1000 K, as this is the suggested high-temperature limit of the method. [54] Current efforts are focused on estimation of other relevant properties (e.g., heat of formation and Gibbs energy of formation) to produce coefficients compatible with **Eqs. (3.2-3.4)** and subsequent incorporation of the data into CEA software.

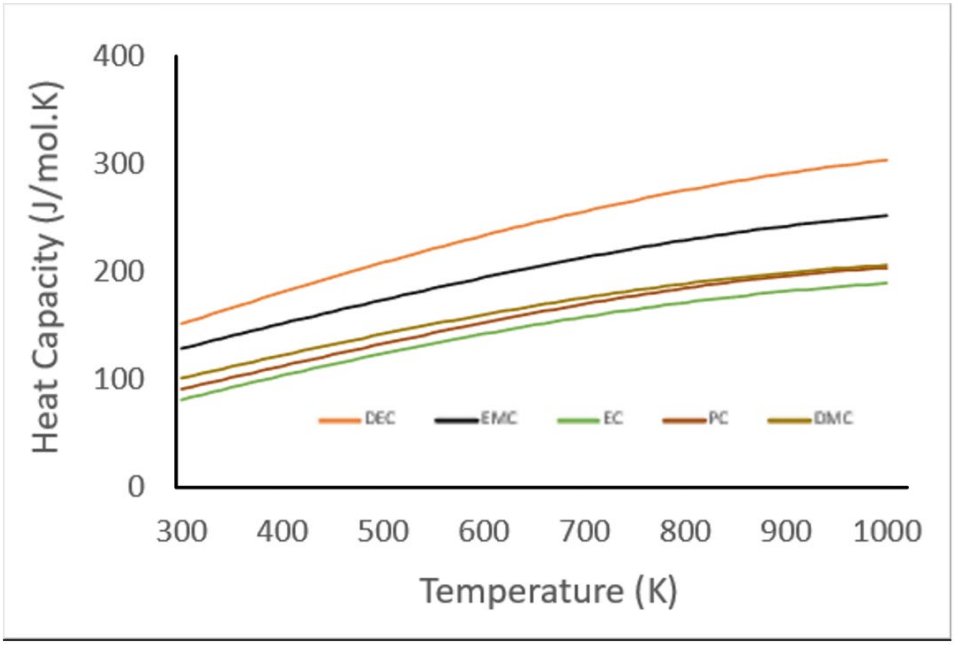

Figure 3.3. *Temperature-dependent specific heat capacities for common LIB electrolytes (EMC, EC, PC, DMC, and DEC) as computed with the Joback method [54].*

3.4 Oxygen Release in Metal Oxide Cathodes

LIB cathodes are generally composed of metal oxides which may or may not be lithiated based on the cells SOC. At elevated temperature, these materials partially decompose and release some, but generally not all their oxygen. One potential drawback of CEA analyses is that the first computational step is dissociation of all reactant compounds into their constituent atoms. However, since LIB cathode materials do not fully decompose at relevant temperatures, this computational method is inaccurate. Accordingly, 'restrictive' modeling must be implemented in the current modeling approach. The authors acknowledge this shortcoming of most CEA software and have acquired a software (LLNL Cheetah 8.0) which will allow for implementation of these restrictions by imposing final concentrations of certain reactants and/or products. This topic is the subject of future work.

3.5 Modeling Approach and Validation Techniques

Most of the modeling efforts completed thus far have focused on key CEA modeling inputs, such as prediction of electrolyte densities for computing product mass/molar concentrations, compilation of relevant reactant heats of formation, and integration of temperature-dependent thermodynamic data of potential electrolyte product species not previously incorporated in CEA software. These are efforts are still underway but are nearing completion. Upon their completion, our team will begin to focus on application of our CEA modeling approach via Praqsys's Cequel software which enable CEA computations within a Microsoft Excel framework. Calculations will be completed assuming a constant-pressure, constant-enthalpy basis, which is consistent with an adiabatic, open-volume system at constant pressure that emulates rapid TR and combustion of LIB cells.

Initial CEA computations will focus on electrolyte solution decomposition for which several key datasets have been established within the literature, as presented within the review in Chapter 2. Our CEA modeling approach will be benchmarked against these electrolyte experiments by comparison of total heat release, total gas release, and gas composition. Subsequently, exploratory studies will be completed to evaluate the effects of varying electrolyte and/or salt composition.

Initial validation of the CEA modeling approach will be followed by extension of the model to full LIB cell chemistries including all components of standard batteries. Additional considerations will include 'restrictive' modeling to regulate expected decomposition and oxygen release from metal oxide cathodes, as well as establishing non-reactive conditions for relevant cell components (e.g., cell can and metal collectors). Once again, the extended CEA modeling

approach will be validated against available experimental data, especially those provided by Golubkov et al. [25-26] and Spray et al. [16].

We expect that these efforts will substantiate our claims that a CEA modeling approach is capable of a priori prediction of LIB TR consequences, ultimately providing a useful simulation tool to the battery safety community.

3.6 Potential Exploratory Modeling Studies

The modeling approach suggested herein should eventually yield a simulation tool capable of comprehensive LIB TR prediction capabilities. Although efforts will initially be focused on validation of tool by benchmarking it against data available in the literature, the ultimate goal is to utilize it to inform future LIB designs. Accordingly, several areas where this simulation tool could be applied are briefly discussed, as follows.

- Evaluation of alternative or novel electrolyte and/or salt solutions
- Consideration of atmospheric composition (i.e., air, inert, ISS)
- Determination of pressure (i.e., ambient, vacuum, high atmosphere) effects
- Investigation of standard and potential firefighting agents including comparison of COTS version (e.g., water, sodium bicarbonate, and ammonium phosphate)
- Analysis of electrolyte additives for various purposes (e.g., aging stability, flame retardant, etc.)
- Consideration of alternative cell chemistries, such a solid-state lithium batteries

4. CONCLUSION

A through review of the literature regarding evaluation of LIB TR consequences and severity was presented herein. All the experiments observed in the literature suffered from various drawbacks. Cone and Tewarson calorimeters allow for collection of fundamental measurements (i.e., heat of combustion) and can provide realistic heating rates but lack direct control of ambient gas reaction volumes. Conversely, ARC experiments have direct control of this parameter and allow for straightforward gas compositional analysis but suffer from slow and unrealistic heating rates. Rapid heating in closed vessels with post-experiment gas sampling appears to be the best method available, especially when condensable species are considered in the compositional gas analysis. In addition, thorough pre-experiment cell characterization experiments elucidating cell composition are generally lacking and should be included in future studies when feasible.

Several noteworthy findings demonstrated from these experiments are described, as follows. Total energy release, heat release rates, and toxic gas production relies heavily on the cell chemistry, including the anode and electrolyte composition. The thermal stability of electrolytes varies significantly, and the total energy release of their decomposition strongly relates to their respective atomic compositions. In general, LFP is observed to exhibit the highest thermal stability of all standard cathode materials. Furthermore, the severity of LIB TR consequences increases with the cell's SOC. Toxic gas emissions were noted in most experimental efforts, but likely only pose significant risks for larger format battery packs. However, gas emissions from all cells are highly flammable and produce significant inherit risks during LIB TR venting.

A CEA modeling framework was proposed and discussed for the *a priori* prediction of LIB TR consequences. The modeling approach discussed herein potentially has the capability to predict

total energy release, total gas release, and gas composition for electrolyte decomposition and LIB TR and combustion. Several difficulties of this modeling approach were discussing, including evaluation of electrolyte densities, prediction of temperature-dependent thermodynamic properties for product species, and restrictions required for partially decomposing or non-reacting reactants. An electrolyte solution density model was developed herein which demonstrated good agreement with the compiled but scarce literature data. This density prediction method is being further refined for improved accuracy and extended to multiple component solutions. Standard group additive methods were applied to predict the temperature-dependent thermodynamic properties of standard electrolytes and are being further refined for incorporation into CEA software. Restrictive modeling efforts, especially related to high-temperature metal oxide decomposition and oxygen release, is an area of future work.

Future work will include validation of the proposed modeling approach by benchmarking the model against available literature data for electrolyte decomposition studies and full LIB cell TR experiments. These efforts will ultimately produce a simulation tool capable of informing future LIB designs. Exploratory modeling efforts will be devoted to evaluation of alternative and novel cell or electrolyte chemistries, flame-retardant additives, and fire mitigation strategies. The development of theoretical models containing information from all of these areas will prove beneficial to the growing LIB industry.

REFERENCES

1. Gordon, S. and McBride, B. J., "Computer Program for Calculation of Complex Chemical Equilibrium Compositions and Applications – I. Analysis," *NASA-RP-1311*, 1994.

2. Gordon, S. and McBride, B. J., "Computer Program for Calculation of Complex Chemical Equilibrium Compositions and Applications – II. Users Manual and Program Description," *NASA-RP-1311*, 1994.

3. Feng, X., Ouyang, M., Liu, X., Lu, L., Xia, Y., and He, X., "Thermal Runaway Mechanism of Lithium Ion Battery for Electric Vehicles: A Review," *Energy Storage Materials*, Vol. 10, 2018, pp. 246-267.
doi: 10.1016/j.ensm.2017.05.013

4. Wang, Q., Mao, B., Stoliarov, S. I., and Sun, J., "A Review of Lithium Ion Battery Failure Mechanisms and Fire Prevention Strategies," *Progress in Energy and Combustion Science*, Vol. 73, 2019, pp. 95-131.
doi: 10.1016/j.pecs.2019.03.002

5. Diaz, F., Wang, Y., Weyhe, R., and Friedrich, B., "Gas Generation Measurement and Evaluation during Mechanical Processing and Thermal Treatment of Spent Li-Ion Batteries," *Waste Management*, Vol. 84, 2019, pp. 102-111.
doi: 10.1016/j.wasman.2018.11.029

6. Abraham, D. P., Roth, E. P., Kostecki, R., McCarthy, K., MacLaren, S., and Doughty, D. H., "Diagnostic Examination of Thermally Abused High-Power Lithium-Ion Cells," *Journal of Power Sources*, Vol. 161, No. 1, 2006, pp. 648-657.
doi:10.1016/j.jpowsour.2006.04.088

7. Roth, E. P. and Orendorff, C. J., "How Electrolytes Influence Battery Safety," *The Electrochemical Society Interface*, Vol. 21, No. 2, 2012, pp. 45-49.
doi: 10.1149/2.f04122if

8. Lamb, J., Orendorff, C. J., Roth, E. P., and Langendorf, J., "Studies on the Thermal Breakdown of Common Li-Ion Battery Electrolyte Components," *Journal of The Electrochemical Society*, Vol. 162, No. 10, 2015, pp. 2131-2135.
doi: 10.1149/2.0651510jes

9. Nagasubramanian, G., "Electrical Characteristics of 18650 Li-ion Cells at Low Temperatures," *Journal of Applied Electrochemistry*, Vol. 31, 2001, pp. 99-104.
doi: 10.1023/A:1004113825283

10. Nagasubramanian, G. and Fenton, K., "Reducing Li-ion Safety Hazards through Use of Non-Flammable Solvents and Recent Work at Sandia National Laboratories," *Electrochimica Acta*, Vol. 101, 2013, pp. 3-10.
doi: 10.1016/j.electacta.2012.09.065

11. Doughty, D. H., Roth, P. E., Crafts, C. C., Nagasubramanian, G., Henriksen G., and Amine, K., "Effects of Additives on Thermal Stability of Li Ion Cells," *Journal of Power Sources*, Vol. 161, No. 1, 2005, pp. 116-120.
doi: 10.1016/j.jpowsour.2005.03.170

12. Somandepalli, B. and Biteau, H., "Cone Calorimetry as a Tool for Thermal Hazard Assessment of Li-Ion Cells," *SAE International Journal of Alternative Powertrains*, Vol. 3, No. 2, 2014, pp. 222-233.
doi: 10.4271/2014-01-1838

13. Somandepalli, V., Marr, K., and Horn, Q., "Quantification of Combustion Hazards of Thermal Runaway Failures in Lithium-Ion Batteries," *SAE International Journal of Alternative Powertrains*, Vol. 3, No. 1, 2014, pp. 98-104.
doi: 10.4271/2014-01-1857

14. Spray, R., Marr, K., White, K., Horn, Q., and Somandepalli, V., "Understanding and Mitigating the Downstream Risk from Thermal Run-Away," *NASA Aerospace Battery Workshop*, Huntsville, AL, 2015.

15. Spray, R., Barry, M., Brown, C., and Marr, K., "Understanding Downstream Risk(s) from Battery Thermal Runaway & Designing for Safety," *NASA Aerospace Battery Workshop*, Huntsville, AL, 2017.

16. Spray, R., Barry, M., Vickery, J., and Myers, T., "Understanding How Testing Conditions Affect Hazard Quantification in Lithium-Ion Battery Abuse Tests," *NASA Aerospace Battery Workshop*, Virtual Event, 2020.

17. Roth, E. P., Crafts, C., Doughty, D. H., and McBreen, J., "Advanced Technology Development Program for Lithium-Ion Batteries: Thermal Abuse Performance of 18650 Li-Ion Cells," *SAND 2004-0584*, 2004.
doi: 10.2172/918751

18. Eshetu, G. G., Bertrand, J. P., Lecocq, A., Grugeon, S., Laruelle, S., Armand, M., and Marlair, G., "Fire Behavior of Carbonates-Based Electrolytes Used in Li-Ion Rechargeable Batteries with a Focus on the Role of the LiPF6 and LiFSI Salts," *Journal of Power Sources*, Vol. 269, 2014, pp. 804-811.
doi:10.1016/j.jpowsour.2014.07.065

19. Eshetu, G. G., Grugeon, S., Laruelle, S., Boyanov, S., Lecocq, A., Bertrand, J. P., and Marlair, G., "In-Depth Safety-Focused Analysis of Solvent Used in Electrolytes for Large Scale Lithium Ion Batteries," *Physical Chemistry Chemical Physics*, Vol. 15, 2013, pp. 9145-9155.
doi: 10.1039/c3cp51315g

20. Ringen, S., Lanum, J., and Miknis, F. P., "Calculating the Heating Values from Elemental Composition of Fossil Fuels," *Fuel*, Vol. 58, No. 1, 1979, pp. 69-71.
doi: 10.1016/0016-2361(79)90056-5

21. Boie, W., "Contributions to Pyrotechnic Computations," *Wissenschaftliche Zeitschnift der Technischen Hochshule Dresden*, Vol. 2, 1952, pp. 687.

22. Lecocq, A., Eshetu, G. G., Grugeon, S., Martin, N., Laruelle, S., and Marlair, G., "Scenario-Based Prediction of Li-Ion Batteries Fire-Induced Toxicity," *Journal of Power Sources*, Vol. 316, 2016, pp. 197-206.
doi: 10.1016/j.jpowsour.2016.02.090

23. Ribiere, P., Grugeon, S., Morcrette, M., Boyanov, S., Laruelle, S., and Marlair, G., "Investigation on the Fire-Induced Hazards of Li-Ion Battery Cells by Fire Calorimetry," *Energy and Environmental Science*, Vol. 5, No. 1, 2012, pp. 5271-5280.
doi: 10.1039/C1EE02218K

24. Forestier, C., Lecocq, A., Zantman, A., Grugeon, S., Sannier, L., Marlair, G., and Laruelle, S., "Study of the Role of LiNi1/3Mn1/3Co1/3O2/Graphite Li-Ion Pouch Cells Confinement, Electrolyte Composition and Separator Coating on Thermal Runaway and Off Gas-Toxicity," *Journal of the Electrochemical Society*, Vol. 167, No. 9, 2020, pp. 1-8
doi: 10.1149/1945-7111/ab829e

25. Golubkov, A. W., Fuchs, D., Wagner, J., Wiltche, H., Stangl, C., Fauler, G., Voitic, G., Thaler, A., and Hacker, V., "Thermal-Runaway Experiments on Consumer Li-Ion Batteries with Metal-Oxide and Olivin-Type Cathodes," *RSC Advances*, Vol. 4, 2014, pp. 3633-3642. doi:10.1039/c3ra45748f

26. Golubkov, A. W., Cheikl, S., Planteu, R., Voitic, G., Wiltche, H., Stangl, C., Fauler, G., Thaler, A., and Hacker, V., "Thermal Runaway of Commercial 18650 Li-Ion Batteries with LFP and NCA Cathodes – Impact of State of Charge and Overcharge," *RSC Advances*, Vol. 4, 2015, pp. 57171-57186. doi:10.1039/c5ra05897j

27. Larsson, F., Andersson, P., Blomqvist, P., Loren, A., and Mellander, B. E., "Characteristics of Lithium-Ion Batteries During Fire Tests," *Journal of Power Sources*, Vol. 271, 2014, pp. 414-420. doi: 10.1016/j.jpowsour.2014.08.027

28. Larsson, F., Andersson, P., Blomqvist, P., and Mellander, B. E., "Toxic Fluoride Gas Emissions from Lithium-Ion Battery Fires," *Scientific Reports*, Vol. 7, 2017, pp. 1-13. doi: 10.1038/s41598-017-09784-z

29. Larsson, F., Bertilsson, S., Furlani, M., Albinsson, I., and Mellander, B. E., "Gas Explosions and Thermal Runaways During External Heating Abuse of Commercial Lithium-Ion Graphite-LiCoO2 Cells at Different Levels of Ageing," *Journal of Power Sources*, Vol. 272, 2018, pp. 220-231. doi: 10.1017/j.jpowsour.2017.10.085

30. Liu, X., Stoliarov, S. I., Denlinger, M., Masias, A., and Snyder, K., "Comprehensive Calorimetry of the Thermally-Induced Failure of a Lithium Ion Battery," *Journal of Power Sources*, Vol. 280, 2015, pp. 516-525. doi: 10.1016/j.jpowsour.2015.01.125

31. Liu, X., Stoliarov, S. I., Denlinger, M., Masias, A., and Snyder, K., "Heat Release during Thermally-Induced Failure of a Lithium Ion Battery: Impact of Cathode Composition," *Fire Safety Journal*, Vol. 85, 2016, pp. 10-22. doi: 10.1016/j.firesaf.2016.08.001

32. Said, A. O., Lee, C., Stoliarov, S. I., and Marshall, A. W., "Comprehensive Analysis of Dynamics and Hazards Associated with Cascading Failure in 18650 Lithium Ion Cell Arrays," *Applied Energy*, Vol. 248, 2019, pp.415-428.
doi: 10.1016/j.apenergy.2019.04.141

33. Lee, C., Said, A. O., and Stoliarov, S. I., "Impact of State of Charge and Cell Arrangement on Thermal Runaway Propagation in Lithium Ion Battery Cell Arrays," *Transportation Research Record*, Vo.673, No. 8, 2019, pp. 408-417.
doi: 10.1177/0361198119845654

34. Lee, C., Said, A. O., and Stoliarov, S. I., "Passive Mitigation of Thermal Runaway Propagation in Dense 18650 Lithium Ion Cell Assemblies," *Journal of The Electrochemical Society*, Vol. 167, 2020, pp. 1-10.
doi: 10.1149/1945-7111/ab8978/pdf

35. Said, A. O., Lee, C., and Stoliarov, S. I., "Experimental Investigation of Cascading Failure in 18650 Lithium Ion Cell Arrays: Impact of Cathode Chemistry," *Journal of Power Sources*, Vol. 446, 2020, pp. 1-14.
doi: 10.1016/j.jpowsour.2019.227347

36. Sun, J., Li, J., Zhou, T., Yang, K., Wei, S., Tang, N., Dang, N., Li, H., Qiu, X., and Chen, L., "Toxicity, A Serious Concern of Thermal Runaway from Commercial Li-Ion Battery," *Nano Energy*, Vol. 27, 2016, pp. 313-319.
doi: 10.1016/j.nanoen.2016.06.031

37. Nedjalkov, A., Meyer, J., Kohring, M., Doering, A., Angelmahr, M., Dahle, S., Sander, A., Fischer, A., and Schade, W., "Toxic Gas Emissions from Damaged Lithium Ion Batteries-Analysis and Safety Enhancement Solution," *Batteries*, Vol. 2, No. 1, 2016, pp. 1-10.
doi: 10.3390/batteries2010005

38. Fernandes, Y., Bry, A., and Persis, S., "Identification and Quantification of Gases Emitted During Abuse Tests by Overcharge of a Commercial Li-Ion Battery," *Journal of Power Sources*, Vol. 389, 2018, pp. 106-119.
doi: 10.1016/j.jpowsour.2018.03.034

39. Peng, Y., Yang, L., Ju, X., Liao, B., Ye, K., Li, L., Cao, B., and Ni, Y., "A Comprehensive Investigation on the Thermal and Toxic Hazards of Large Format Lithium-Ion Batteries with LiFePO4 Cathode," *Journal of Hazardous Materials*, Vol. 381, 2020, pp. 1-11.
doi: 10.1016/j.jhazmat.2019.120916

40. Dougassa, Y. R., Tessier, C., Ouatani, L. E., Anouti, M., and Jacquemin, J., "Low Pressure Carbon Dioxide Solubility in Lithium-Ion Batteries Based Electrolytes as a Function of Temperature. Measurement and Prediction," *The Journal of Chemical Thermodynamics*, Vol. 61, 2013, pp. 32-44.
doi:10.1016/j.jct.2012.12.025

41. Su, L., Darling, R. M., Gallagher, K. G., Xie, W., Thelen, J. L., Badel, A. F., Barton, J. L., Cheng, K. J., Balsara, N. P., Moore, J. S., and Brushett, F. R., "An Investigation of the Ionic Conductivity and Species Crossover of Lithiated Nafion 117 in Nonaqueous Electrolytes," *Journal of The Electrochemical Society*, Vol. 163, No. 1, 2015, pp. 1-10.
doi: 10.1149/2.03211601jes

42. Stewart, S. and Newman, J., "Measuring the Salt Activity Coefficient in Lithium-Battery Electrolytes," *Journal of The Electrochemical Society*, Vol. 155, No. 6, 2008, pp. 458-463.
doi: 10.1149/1.2904526

43. Laoire, C. O., Plichta, E., Hendrickson, M., Murkerjee, S., and Abraham, K. M., "Electrochemical Studies of Ferrocene In a Lithium Ion Conducting Organic Carbonate Electrolyte," *Electrochimica Acta*, Vol. 54, No. 26, 2009, pp. 6560-6564.
doi: 10.1016/j.electacta.2009.06.041.

44. Salami, N., "Molecular Dynamics (MD) Study on the Electrochemical Properties of Electrolytes in Lithium-Ion Battery (LIB) Applications," MS Thesis, University of Wisconsin-Milwaukee, 2014.

45. Ong, M. T., Verners, O., Draeger, E. W., Van Duin, A. C. T., Lordi, V., and Pask, J. E., "Lithium Ion Solvation and Diffusion in Bulk Organic Electrolytes from First-Principles and Classical Reactive Molecular Dynamics," *The Journal of Physical Chemistry B*, Vol. 119, No. 4, 2015, pp. 1535-1545.
doi: 10.1021/jp508184f

46. Hou, T. and Monroe, C. W., "Composition-Dependent Thermodynamic and Mass-Transport Characterization of Lithium Hexafluorophosphate in Propylene Carbonate," *Electrochimica Acta*, Vol. 332, 2020, pp. 1-15.
doi: 10.1016/jelectacta.2019.135085

47. Wang, A. A., Hou, T., Karanjavala, M., and Monroe, C. W., "Shifting-Reference Concentration Cells to Refine Composition-Dependent Transport Characterization of Binary Lithium-Ion Electrolytes," *Electrochimica Acta*, Vol. 358, 2020, pp. 136688. doi: 10.1016/j.electacta.2020.136688

48. Lam, E. J., Alvarez, M. N., Galvez, M. E., and Alvarez, E. B., "A Model for Calculating the Density of Aqueous Multicomponent Electrolyte Solutions," *Journal of the Chilean Chemical Society*, Vol. 52, No. 1, 2008, pp. 1393-1398. doi: 10.4067/S0717-97072008000100015

49. Horsák, I. and Sláma, I., "Densities of Aqueous Electrolyte Solutions. A Model for a Data Bank," *Journal of Chemical and Engineering Data*, Vol. 31, No. 4, 1986, pp. 434-437. doi: 10.1021/je00046a018

50. Gavritchev, K. S., Sharpataya, G. A., Smagin, A. A., Malyi, E. N., and Matyukha, V. A., "Calorimetric Study of Thermal Decomposition of Lithium Hexafluorophosphate," *Journal of Thermal Analysis and Calorimetry*, Vol. 73, 2003, pp. 71-83. doi: 10.1023/A:1025125306291

51. Zinigrad, E., Larush-Asraf, L., Gnanaraj, J. S., Sprecher, M., and Aurbach, D., "On the Thermal Stability of $LiPF_6$," *Thermochimica Acta*, Vol. 438, No. 1-2, 2005, pp. 184-191. doi: 10.1016/j.tca.2005.09.006

52. Iyer, R. G., Delacourt, C., Masquelier, C., Tarascon, J. M., and Navrotsky, A., "Energetics of $LiFePO_4$ and Polymorphs of Its Delithiated Form, $FePO_4$," *Electrochemical and Solid-State Letters*, Vol. 9, No. 2, 2006, pp. 46-48. doi: 10.1149/1.2140496

53. Roder, P., Baba, N., Friedrich, K. A., and Wiemhofer, H. D., "Impact of Delithiated Li_0FePO_4 on the Decomposition of LiPF6-Based Electrolyte Studied by Accelerating Rate Calorimetry," *Journal of Power Sources*, Vol. 236, 2013, pp. 151-157. doi: 10.1016/j.jpowsour.2013.02.044

54. Joback, K. G. and Reid, R. C., "Estimation of Pure-Component properties from Group-Contributions," *Chemical Engineering Communications*, Vol. 57 No. 2, 1987, pp. 233-243. doi: 10.1080/00986448708960487

55. Kleiber, M. and Joh, R., *VDI Heat Atlas*, 2nd ed., "Section D1: Calculation Methods for Thermophysical Properties," Springer-Verlag Berlin Heidelberg, 2010.

APPENDIX A

Permission to Utilize Feng et. al.'s Figure

ELSEVIER LICENSE
TERMS AND CONDITIONS

Jan 28, 2021

This Agreement between Texas A&M University -- James Thomas ("You") and Elsevier ("Elsevier") consists of your license details and the terms and conditions provided by Elsevier and Copyright Clearance Center.

License Number	4983540564764
License date	Jan 07, 2021
Licensed Content Publisher	Elsevier
Licensed Content Publication	Energy Storage Materials
Licensed Content Title	Thermal runaway mechanism of lithium ion battery for electric vehicles: A review
Licensed Content Author	Xuning Feng,Minggao Ouyang,Xiang Liu,Languang Lu,Yong Xia,Xiangming He
Licensed Content Date	Jan 1, 2018
Licensed Content Volume	10
Licensed Content Issue	n/a

Licensed Content Pages	22
Start Page	246
End Page	267
Type of Use	reuse in a journal/magazine
Requestor type	academic/educational institute
Portion	figures/tables/illustrations
Number of figures/tables/illustrations	1
Format	electronic
Are you the author of this Elsevier article?	Yes
Will you be translating?	No
Title of new article	A Priori Modeling of Thermal Runaway Consequences in Lithium-Ion Batteries
Title of targeted journal	Journal of Power Sources
Publisher	Elsevier
Expected publication date	Jan 2022
Portions	Figure 10
Requestor Location	Texas A&M University 1485 George Bush Drive West COLLEGE STATION, TX 77843 United States Attn: Texas A&M University